

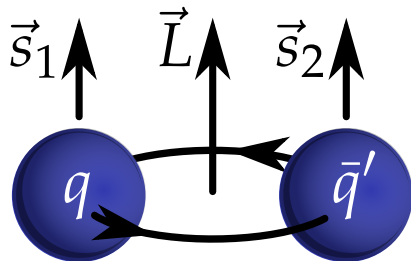
Studies of light mesons at COMPASS

Sebastian Uhl
On Behalf of the COMPASS Collaboration



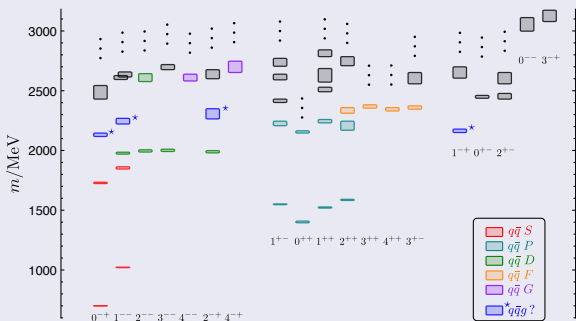
PANIC2014 28.08.2014

- Quark spins couple to total intrinsic spin $S = 0$ (singlet) or 1 (triplet)
- Relative orbital angular momentum \vec{L} and total spin \vec{S} couple to meson spin $\vec{J} = \vec{L} + \vec{S}$
- parity $P = (-1)^{L+1}$
- charge conjugation $C = (-1)^{L+S}$
- forbidden J^{PC} :
 $0^{--}, 0^{+-}, 1^{-+}, 2^{+-}, 3^{-+}, \dots$



Naïve Constituent Quark Model

- Quark spins couple to total spin $S = 0$ (singlet) or 1 (triplet)
- Relative orbital angular momentum and total spin \vec{S} couple to meson spin $\vec{J} = \vec{L} + \vec{S}$
- parity $P = (-1)^{L+1}$
- charge conjugation $C = (-1)^{L+S}$
- forbidden J^{PC} : $0^{--}, 0^{+-}, 1^{-+}, 2^{+-}, 3^{--}$



J.Dudek, Phys.Rev.D84 (2011) 074023

Beyond the CQM: i.e. lattice QCD

isovector states

- prediction of states outside CQM
- hybrid candidate ($q\bar{q}g$)
- lightest candidate in 1^{-+}

in addition:

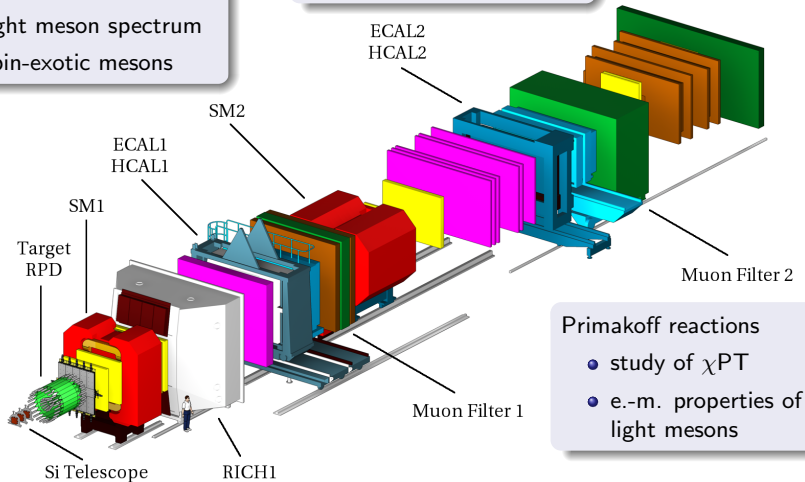
- (isoscalar) glueballs
- pure glue
- quantum numbers J^{PC} : $0^{++}, \dots$

diffractive dissociation

- light meson spectrum
- spin-exotic mesons

central production

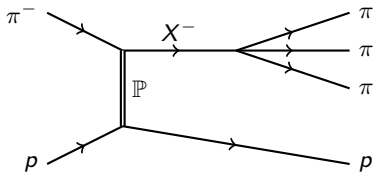
- glue-rich environment
- scalar resonances



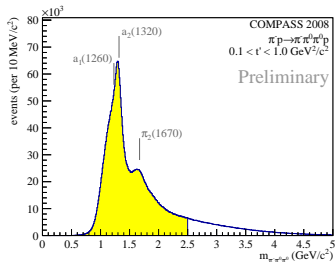
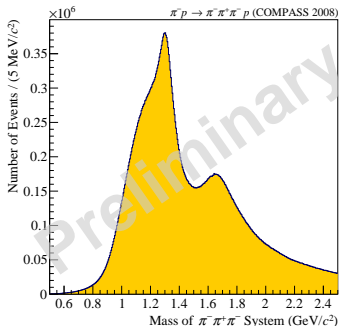
Primakoff reactions

- study of χ PT
- e.-m. properties of light mesons

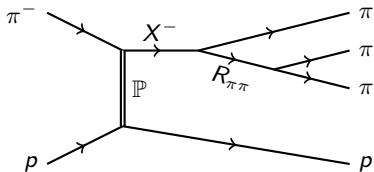
$$\pi^- p \rightarrow (3\pi)^- p$$



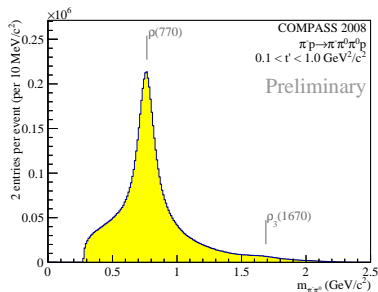
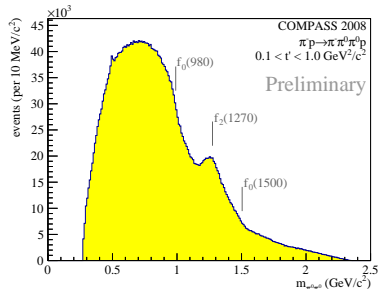
- 190 GeV/c π^- beam on ℓH_2 target
- exclusive $\pi^- p \rightarrow (3\pi)^- p$ reaction
- two channels in COMPASS
 - $\pi^- \pi^- \pi^+$
 - $\pi^- \pi^0 \pi^0$
- high- t' region: $0.1 < t' < 1.0 \text{ GeV}^2/c^2$
- huge dataset
 - 50 million $\pi^- \pi^- \pi^+$ events
 - 3.5 million $\pi^- \pi^0 \pi^0$ events

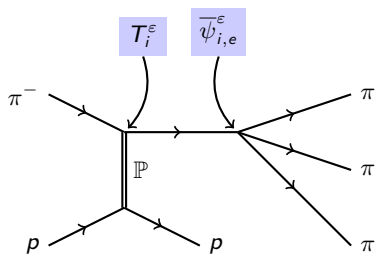


$$\pi^- p \rightarrow (3\pi)^- p$$

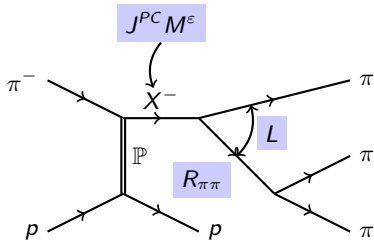


- 190 GeV/c π^- beam on ℓH_2 target
- exclusive $\pi^- p \rightarrow (3\pi)^- p$ reaction
- two channels in COMPASS
 - $\pi^- \pi^- \pi^+$
 - $\pi^- \pi^0 \pi^0$
- high- t' region: $0.1 < t' < 1.0 \text{ GeV}^2/c^2$
- huge dataset
 - 50 million $\pi^- \pi^- \pi^+$ events
 - 3.5 million $\pi^- \pi^0 \pi^0$ events
- partial-wave analysis using isobar model



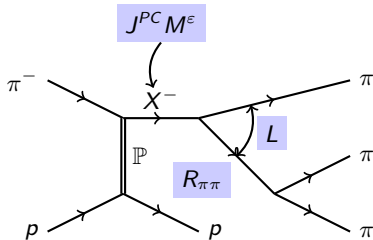


- process can be factorized
 - production T_i^ε
 - decay $\overline{\psi}_{i,e}^\varepsilon$



- process can be factorized
 - production T_i^ϵ
 - decay $\bar{\psi}_{i,e}^\epsilon$
- two-step approach
- 1 fit in mass and t' bins
 - extract production amplitudes T_i^ϵ

- 88 waves
 - 80 with positive reflectivity
 - 7 with negative reflectivity
 - flat wave
- spin J up to 6
- angular momentum L between bachelor π and isobar up to 6
- used isobars:
 - with isospin $I = 0$:
 $(\pi\pi)_S$, $f_0(980)$, $f_2(1270)$, $f_0(1500)$
 - with isospin $I = 1$:
 $\rho(770)$, $\rho_3(1690)$
- for $\pi^- \pi^- \pi^+$ all isobars are $\pi^- \pi^+$
- for $\pi^- \pi^0 \pi^0$:
 - $I = 0$ in $\pi^0 \pi^0$
 - $I = 1$ in $\pi^- \pi^0$

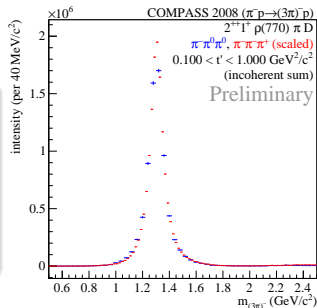
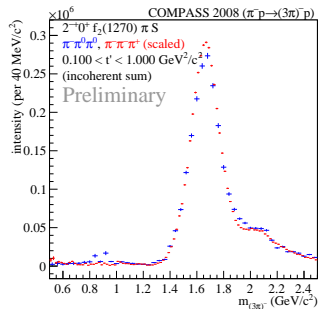
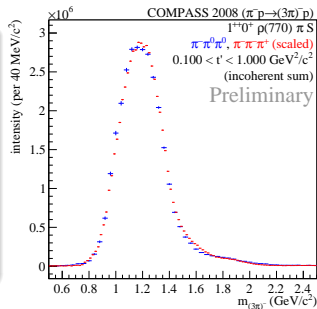


- process can be factorized
 - production T_i^{ϵ}
 - decay $\bar{\psi}_{i,e}^{\epsilon}$
- two-step approach
- 1 fit in mass and t' bins
 - extract production amplitudes T_i^{ϵ}
- 2 fit of mass dependence of spin-density matrix
 - extract resonance parameters

- 88 waves
 - 80 with positive reflectivity
 - 7 with negative reflectivity
 - flat wave
- spin J up to 6
- angular momentum L between bachelor π and isobar up to 6
- used isobars:
 - with isospin $I = 0$:
 $(\pi\pi)_S$, $f_0(980)$, $f_2(1270)$, $f_0(1500)$
 - with isospin $I = 1$:
 $\rho(770)$, $\rho_3(1690)$
- for $\pi^- \pi^- \pi^+$ all isobars are $\pi^- \pi^+$
- for $\pi^- \pi^0 \pi^0$:
 - $I = 0$ in $\pi^0 \pi^0$
 - $I = 1$ in $\pi^- \pi^0$

major waves

- $1^{++}0^+ \rho(770) \pi S$
- $2^{-+}0^+ f_2(1270) \pi S$
- $2^{++}1^+ \rho(770) \pi D$



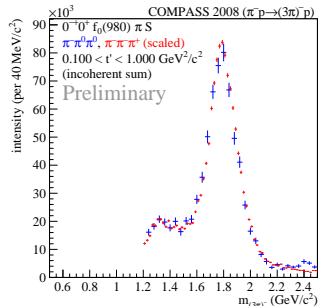
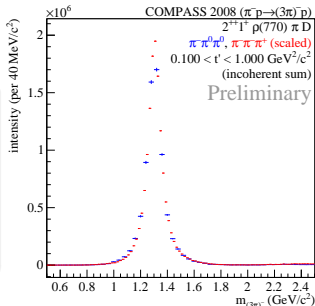
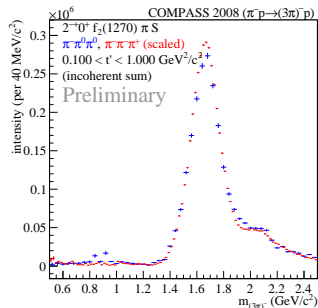
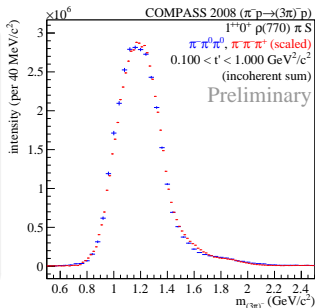
- $\pi^- \pi^0 \pi^0$
- $\pi^- \pi^- \pi^+$ (scaled)
- scaled for each plot
- good agreement between channels

major and minor waves

- $1^{++}0^+ \rho(770) \pi S$
- $2^{-+}0^+ f_2(1270) \pi S$
- $2^{++}1^+ \rho(770) \pi D$
- $0^{-+}0^+ f_0(980) \pi S$

stable fits also for small waves

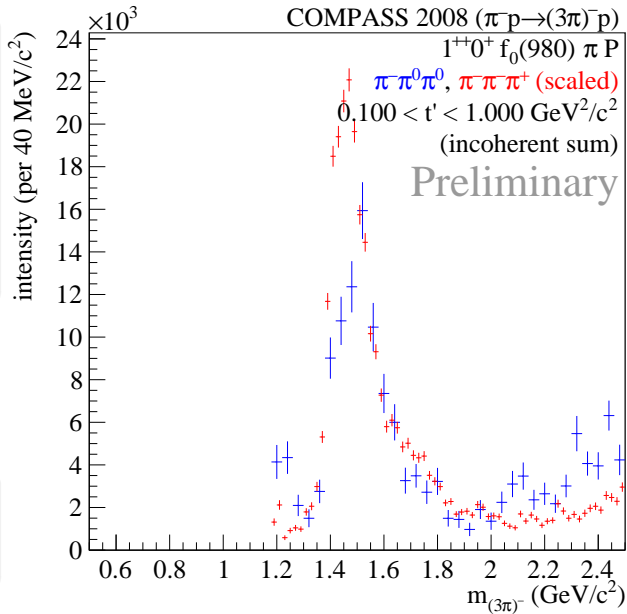
- $\pi^- \pi^0 \pi^0$
- $\pi^- \pi^- \pi^+$ (scaled)
- scaled for each plot
- good agreement between channels



$f_0(980)$ isobar

- $1^{++}0^+ f_0(980) \pi P$
- stable fits also for small waves
- first observation of a signal in $1^{++}0^+ f_0(980) \pi P$ around $1.4 \text{ GeV}/c^2$

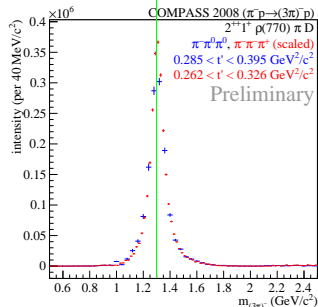
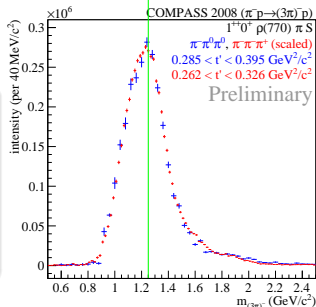
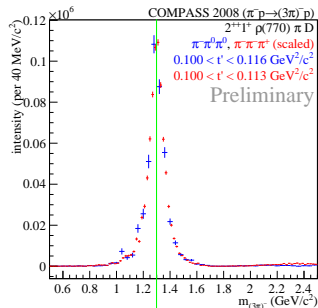
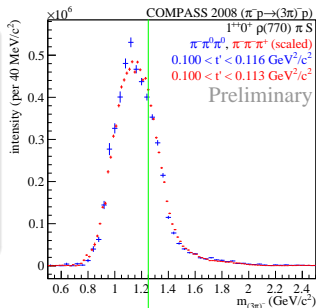
- $\pi^- \pi^0 \pi^0$
- $\pi^- \pi^- \pi^+$ (scaled)
- scaled for each plot



Mass-independent fit

different t' bins

- $1^{++}0^+ \rho(770) \pi S$
- $2^{++}1^+ \rho(770) \pi D$
- position of peak in $1^{++}0^+$ changes
- a_2 not affected



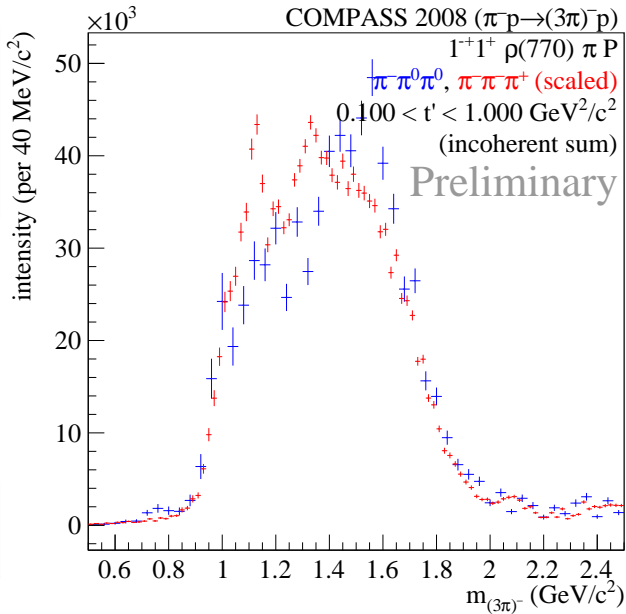
- $\pi^- \pi^0 \pi^0$
- $\pi^- \pi^- \pi^+$ (scaled)
- scaled for each plot
- good agreement between channels

$1^{-+}1^{+}\rho(770)\pi P$

complete t' range

- some differences between channels
- no clear $\pi_1(1600)$ peak

- $\pi^{-}\pi^0\pi^0$
- $\pi^{-}\pi^{-}\pi^{+}$ (scaled)
- scaled for each plot



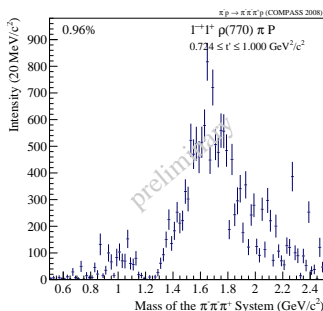
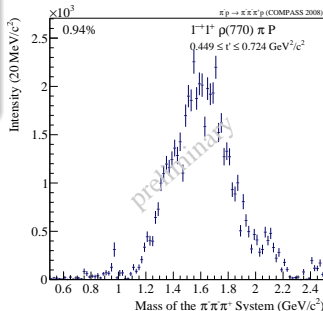
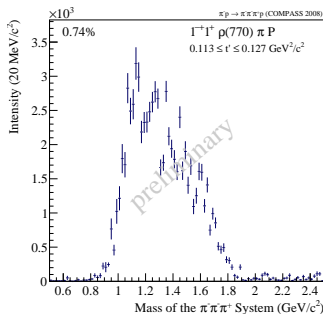
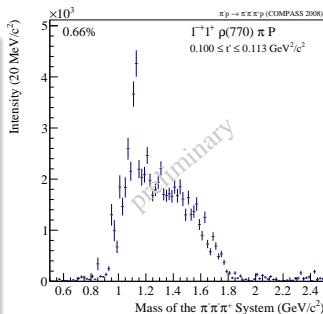
$1^{-+}1^{+}\rho(770)\pi P$

complete t' range

- some differences between channels
- no clear $\pi_1(1600)$ peak

individual t' bins

- peak at $1.6 \text{ GeV}/c^2$ at higher t'
- non-resonant contribution at low t'



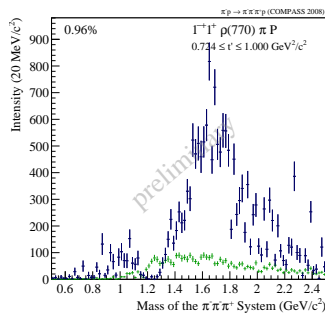
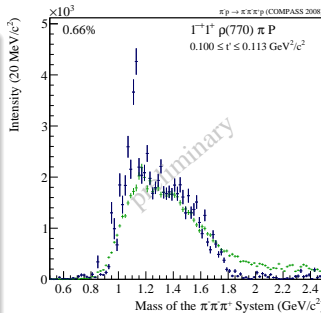
$1^{-+}1^{+}\rho(770)\pi P$

complete t' range

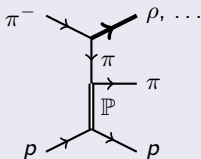
- some differences between channels
- no clear $\pi_1(1600)$ peak

individual t' bins

- peak at $1.6 \text{ GeV}/c^2$ at higher t'
- non-resonant contribution at low t'



Deck effect



- Deck model projected to individual waves
- scaled to the sum of intensities over all t' bins for each wave
- large contribution at low t' predicted for $1^{-+}1^{+}\rho(770)\pi P$

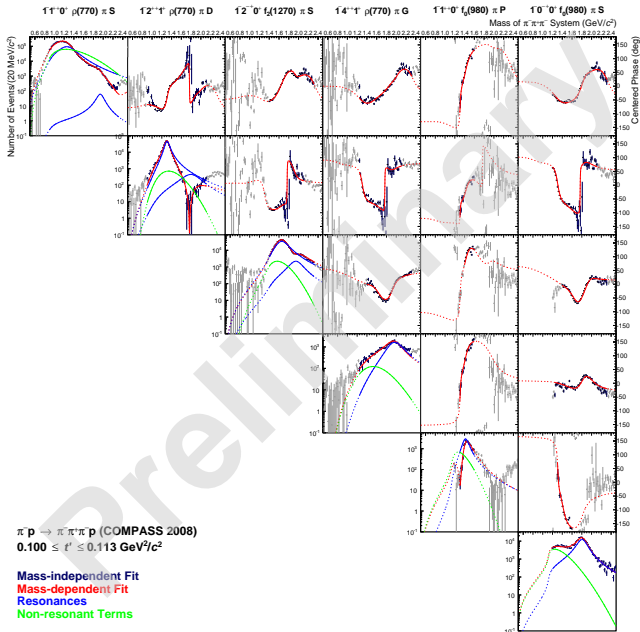
Model

- for the moment six waves
 - three major waves and three smaller waves
- describe spin-density sub-matrix with Breit-Wigner functions

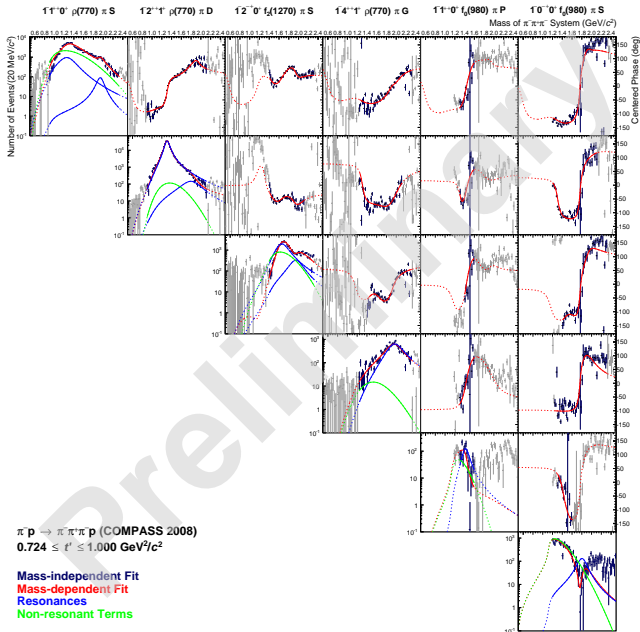
$1^{++}0^+ \rho(770) \pi S$	two BW:	$a_1(1260), a'_1$
$2^{-+}0^+ f_2(1270) \pi S$	two BW:	$\pi_2(1670), \pi_2(1880)$
$2^{++}1^+ \rho(770) \pi D$	two BW:	$a_2(1320), a'_2$
$4^{++}1^+ \rho(770) \pi G$	one BW:	$a_4(2040)$
$1^{++}0^+ f_0(980) \pi P$	one BW:	$a_1(1420)$
$0^{-+}0^+ f_0(980) \pi S$	one BW:	$\pi(1800)$

- non-resonant term for each wave
- extract resonance parameters from all 11 t' bins simultaneously
 - same resonance parameters in all bins
 - couplings may vary
- 352 free parameters, around 15 000 data points

Mass-dependent fit for $\pi^- \pi^- \pi^+$



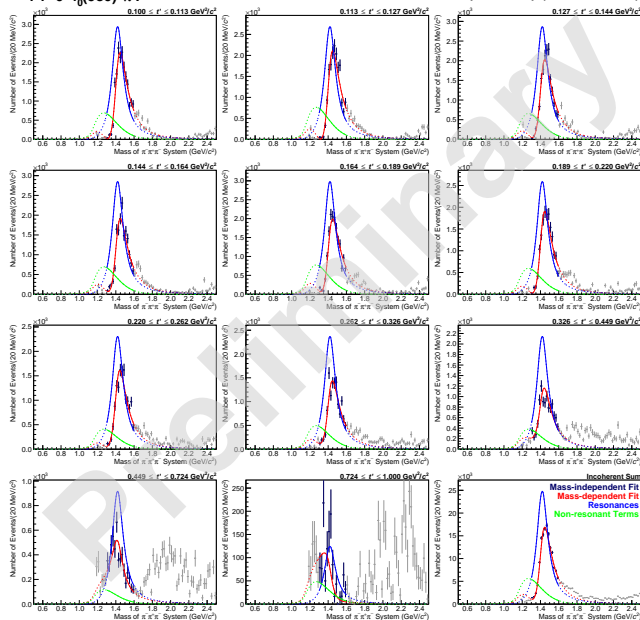
Mass-dependent fit for $\pi^- \pi^- \pi^+$



Mass-dependent fit of $1^{++}0^+ f_0(980) \pi P$

$\Gamma 1^{++}0^+ f_0(980) \pi P$

$\pi^+ p \rightarrow \pi^+ \pi^+ \pi^+ p$ (COMPASS 2008)



- for new $a_1(1420)$
- mass
1412 – 1422 MeV/c²
 - width
130 – 150 MeV/c²
 - well determined
 - narrow

COMPASS is a precision experiment to study light mesons

- unchallenged dataset for $\pi^- \pi^- \pi^+$
- charged and neutral particles with the same experimental setup

partial-wave analysis is a versatile tool for spectroscopy

- various channels under study
- t' -resolved analysis, first mass-dependent fit in 11 t' bins
- new resonance $a_1(1420)$:
 - $M_{a_1(1420)} = 1412 - 1422 \text{ MeV}/c^2$, $\Gamma_{a_1(1420)} = 130 - 150 \text{ MeV}/c^2$
 - $\sim 180^\circ$ phase motion with respect to reference waves
- detailed study of the 1^{-+} state ($\pi_1(1600)$)

further analyses in the COMPASS hadron program

- spectroscopy also in central production reactions
- measurement of radiative width of $a_2(1320)$ and $\pi_2(1670)$
- measurement of π polarizability and other tests of χ PT
- measurement of OZI violation

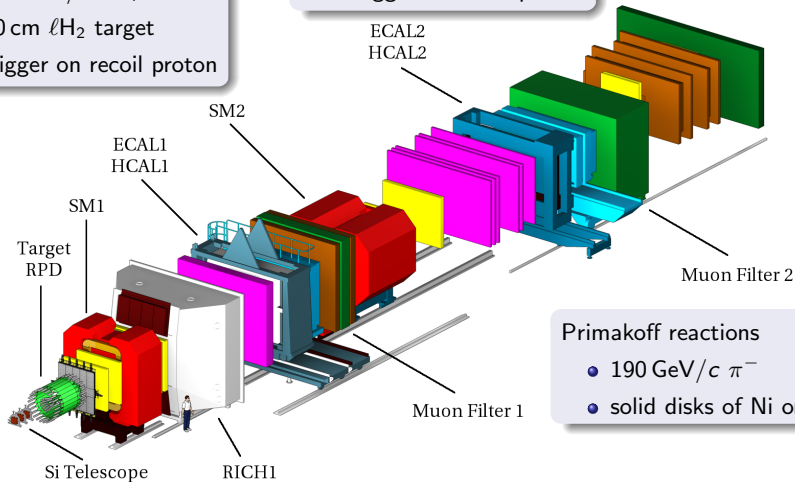
Backup

diffractive dissociation

- 190 GeV/c π^- , K^-
- 40 cm ℓH_2 target
- trigger on recoil proton

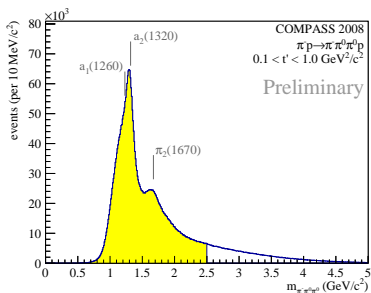
central production

- 190 GeV/c p
- 40 cm ℓH_2 target
- trigger on recoil proton

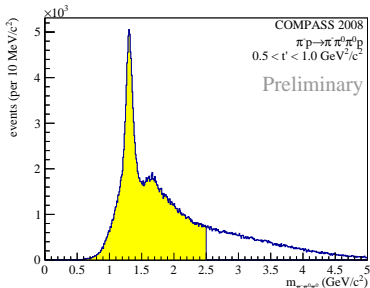
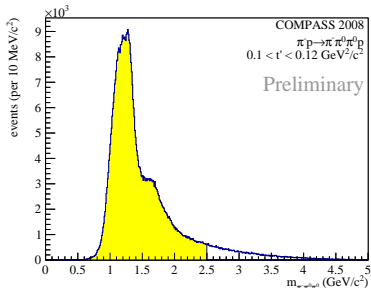


Primakoff reactions

- 190 GeV/c π^-
- solid disks of Ni or Pb



- mass spectrum depends on t'
- at low- t' ($0.1 < t' < 0.2 \text{ GeV}^2/c^2$)
 - $a_1(1260)$ dominates low-mass region
 - $a_2(1320)$ hardly visible
- at high- t' ($0.5 < t' < 1.0 \text{ GeV}^2/c^2$)
 - $a_1(1260)$ visible only as a shoulder
 - $a_2(1320)$ dominant
- no changes above $\pi_2(1670)$ region
- binning of data also in t'
 - 11 bins for $\pi^- \pi^- \pi^+$
 - 8 bins for $\pi^- \pi^0 \pi^0$



data binned

- in 50 mass bins of $40 \text{ MeV}/c^2$ width
- in 8 t' bins with equal amount of statistics

in each mass and t' bin optimize

$$\log \mathcal{L} = - \sum_e^{\text{RD evts.}} \log \left(\sum_{\varepsilon}^{\text{refl.}} \left| \sum_i^{\text{waves}} T_i^{\varepsilon} \cdot \bar{\psi}_{i,e}^{\varepsilon} \right|^2 \right) + \sum_{\varepsilon}^{\text{refl.}} \left(\sum_{i,j}^{\text{waves}} T_i^{\varepsilon} \cdot (T_j^{\varepsilon})^* \cdot \bar{\mathcal{A}}_{ij}^{\varepsilon} \right)$$

Spin-density matrix

$$\rho_{ij}^{\varepsilon} = T_i^{\varepsilon} \cdot (T_j^{\varepsilon})^*$$

intensity

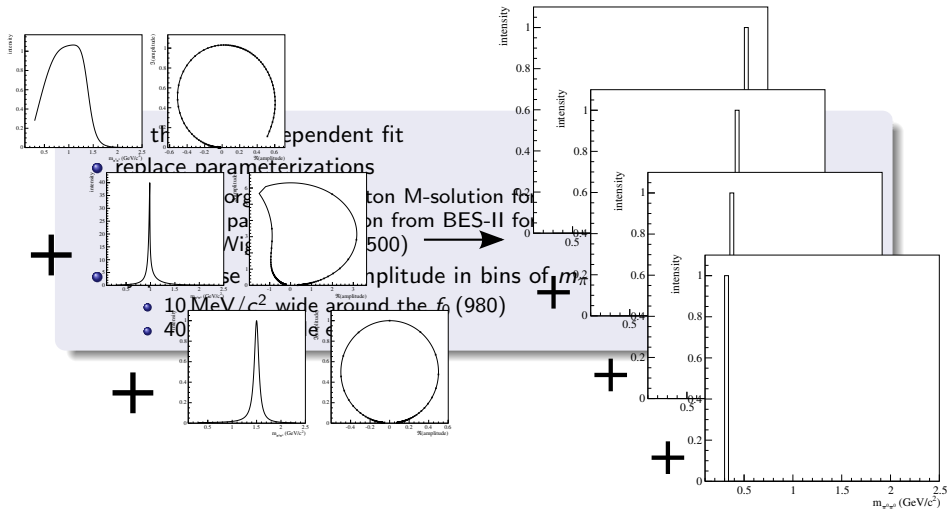
$$I_i^{\varepsilon} = \rho_{ii}^{\varepsilon}$$

absolute value and phase

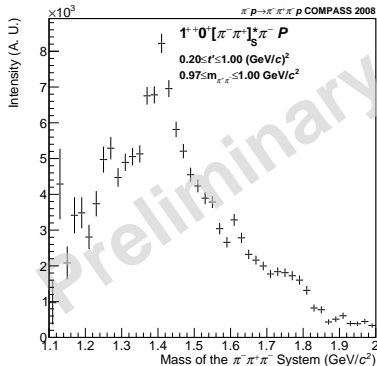
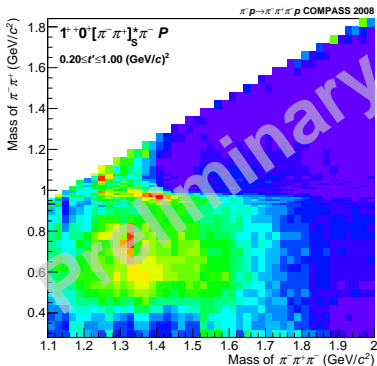
$$\rho_{ij}^{\varepsilon} = r_{ij}^{\varepsilon} e^{i \cdot \varphi_{ij}^{\varepsilon}}$$

- for the mass-independent fit
- replace parameterizations
 - Au, Morgen, Pennington M-solution for $(\pi\pi)_S$ wave
 - Flatté parameterization from BES-II for $f_0(980)$
 - Breit-Wigner for $f_0(1500)$
- by piecewise constant amplitude in bins of $m_{\pi\pi}$
 - 10 MeV/ c^2 wide around the $f_0(980)$
 - 40 MeV/ c^2 wide elsewhere

Extraction of $(\pi\pi)_S$ wave from data



- for the mass-independent fit
 - replace parameterizations
 - Au, Morgen, Pennington M-solution for $(\pi\pi)_S$ wave
 - Flatté parameterization from BES-II for $f_0(980)$
 - Breit-Wigner for $f_0(1500)$
 - by piecewise constant amplitude in bins of $m_{\pi\pi}$
 - 10 MeV/ c^2 wide around the $f_0(980)$
 - 40 MeV/ c^2 wide elsewhere
-
- increase in number of fit parameters
 - requires a lot of data
 - only done for 0^{-+} , 1^{++} , 2^{-+}

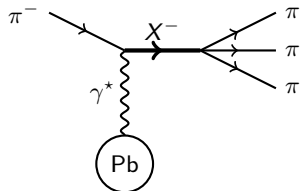


application to 1^{++}

- high- t' : $0.2 < t' < 1.0 \text{ GeV}^2/c^2$
- select $m_{2\pi}$ region around f_0 (980)
- correlation of a_1 (1420) with f_0 (980)

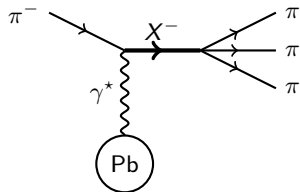
- decay $X \rightarrow \pi\gamma$ allows access to electromagnetic transitions
 - $a_2(1320) \rightarrow \pi\gamma$ magnetic quadrupole moment
 - $\pi_2(1670) \rightarrow \pi\gamma$ electric quadrupole moment
- direct measurement of $\pi\gamma$ decay is experimentally challenging
- inverse process: scattering of a π off a Coulomb potential
 - quasi-real photons in the vicinity of heavy nuclei
- cross-section for Primakoff produced X

$$\sigma_{\text{Primakoff},X} \propto \Gamma_0(X \rightarrow \pi\gamma)$$



- decay $X \rightarrow \pi\gamma$ allows access to electromagnetic transitions
 - $a_2(1320) \rightarrow \pi\gamma$ magnetic quadrupole moment
 - $\pi_2(1670) \rightarrow \pi\gamma$ electric quadrupole moment
- direct measurement of $\pi\gamma$ decay is experimentally challenging
- inverse process: scattering of a π off a Coulomb potential
 - quasi-real photons in the vicinity of heavy nuclei
- cross-section for Primakoff produced X

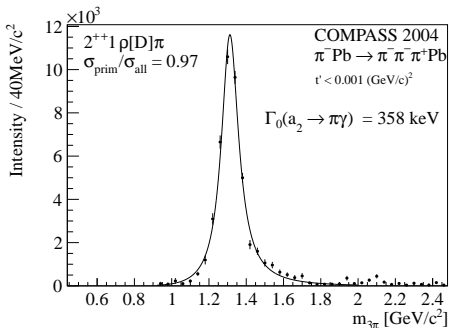
$$\sigma_{\text{Primakoff},X} \propto \Gamma_0(X \rightarrow \pi\gamma)$$



identify Primakoff contribution

- Primakoff produced states have spin projection $M = 1$
- cross-section for diffractively produced states

$$\sigma \propto t'^M e^{-bt'}$$
- at small t' $M = 1$ states are predominantly Primakoff produced
- partial-wave analysis to identify the $M = 1$ final states
- get cross-section from partial-wave intensity



EPJ A Highlight: EPJ A 50: 79 (2014)

radiative width

- for a_2 (1320):
(358 ± 6 ± 42) keV
- for π_2 (1670):
(181 ± 11 ± 27) keV

first measurement

